ORIGINAL PAPER

Binary Phase Behavior of Diacid 1,3-Diacylglycerols

R. John Craven · Robert W. Lencki

Abstract Fifteen phase diagrams were prepared using data from differential scanning calorimetry analysis of binary blends of representative diacid 1,3-DAG. The behavior observed in binary phase diagrams is related to the difference in T_m (ΔT_m) between system components—eutectic for $\Delta T_m < 26$ °C and monotectic for $\Delta T_m > 30$ °C. Binary blends were prepared using six diacid 1,3-DAG: 1,3-hexanoyl-lauroyl-*rac*-glycerol, 1,3-hexanoyl-palmitoyl-*rac*-glycerol, 1,3-hexanoyl-oleoyl-*rac*-glycerol, 1,3-lauroyl-palmitoyl-*rac*-glycerol, 1,3-lauroyl-oleoyl-*rac*-glycerol and 1,3-palmitoyl-oleoyl-*rac*-glycerol. Diacid 1,3-DAG were synthesized using representative FA: hexanoic (6:0)—short-chain FA; lauric (12:0)—medium-chain FA; palmitic (16:0)—long-chain FA; and oleic (18:1)—mono-unsaturated FA. In addition to the aforementioned phase diagrams, the physical chemistry of 1,3-hexanoyl-lauroyl-*rac*-glycerol, 1,3-hexanoyl-oleoyl-*rac*-glycerol and 1,3-lauroyl-oleoyl-*rac*-glycerol is reported.

Keywords 1,3-Diacylglycerol · Phase diagram · Thermal analysis · Polymorphism

Introduction

In nature and industry, chemical components are rarely produced or used in isolation. For instance, natural fats and oils are mixtures of acylglycerols (predominantly triacylglycerols) and any commercially-prepared structured or synthetic lipid (present or future) will probably have a mixed composition. For this reason, compounds in any lipid class cannot be considered completely characterized until the phase behavior of their mixtures is understood. To this end, simple phase diagrams for binary mixtures of pure homologues should be derived first. In due course, the information they provide can be brought to bear on more complex systems containing non-homologous molecules.

The melting behavior of binary mixtures has been investigated for many lipid classes. The phase behavior of mixtures of pure triacylglycerols (TAG) [1–3], fatty acids (FA) [4, 5] and naturally occurring neutral and polar lipids such as TAG [1, 6] and phospholipid [7] have been studied. The phase behavior of binary blends of monoacid esters of 1,3-propanediol, which have a structural resemblance to 1,3-diacylglycerols (1,3-DAG), has also been examined [8–10]. 1,3-DAG are present in many food systems including some specifically designed for weight-loss [11]. Consequently, their phase behavior is of interest. Yet, to date, there have been no published studies detailing the phase behavior of mono- or diacid 1,3-DAG.

The melting data necessary for the compilation of phase diagrams can be obtained using thermal techniques such as differential scanning calorimetry (DSC) and differential thermal analysis (DTA). In lipids, thermal analysis and calorimetry have been used to derive phase diagrams for binary TAG either by calculating solid fat index from DTA data [6] or, more commonly, by directly recording both the start and end of melting [2, 3]. Also in the area of lipid chemistry, binary mixtures of FA have been studied and phase diagrams have been constructed using DSC melting data for 18:1/18:0 and 18:1/22:0 [5], 18:1/12:0, 18:1/14:0 and 18:1/16:0 [12], 18:1/10:0 and 18:1/8:0 [13], as well as 18:1 acid with 18:1 alcohol [4]. Beyond lipid chemistry, thermal techniques have also been used to study complex interactions of commercial and technical significance such

R. J. Craven · R. W. Lencki (✉)
Department of Food Science, University of Guelph, Guelph, ON N1G 2W1, Canada
e-mail: rlencki@uoguelph.ca

Fig. 1 Main types of phase diagrams are **a** continuous solid solution, **b** eutectic, **c** monotectic, partial solid solution, **d** peritectic
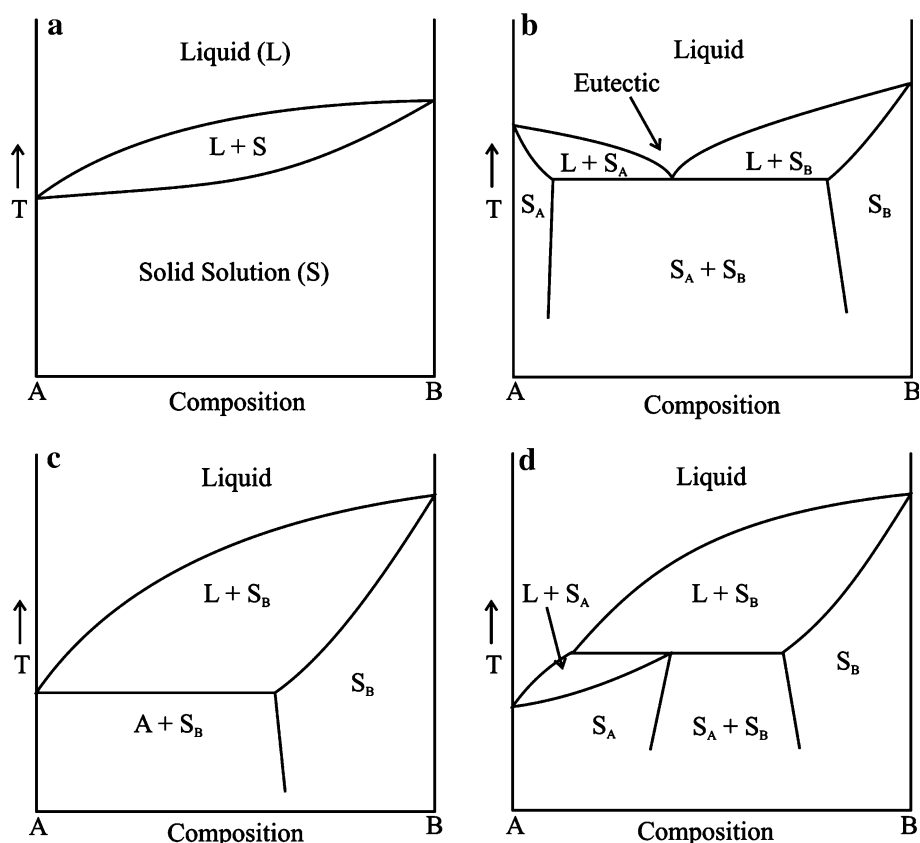
as the storage stability and formulation characteristics of pharmaceutical products (e.g. ibuprofen and stearic acid [14]), the production and properties of fabrics and polymers (e.g. cellulose solvent and water mixtures [15]) and several illustrative eutectic systems [16–19].

Fifteen phase diagrams were prepared using DSC melting data for binary mixtures of six model diacid 1,3-DAG. Model 1,3-DAG were synthesized with representative FA: hexanoic (6:0)—short-chain FA (SCFA); lauric (12:0)—medium-chain FA (MCFA); palmitic (16:0)—long-chain FA (LCFA); and oleic (18:1)—mono-unsaturated FA (MUFA). These compounds have a wide range of melting points due to their varied composition. As a result, it is possible to ascertain the role of melting point difference (ΔT_m) in binary phase behavior of 1,3-DAG. In addition, because some binary mixtures have FA in common (12 mixtures) and others do not (3 mixtures) it may be possible to determine the role of compositional similarity on phase behavior.

Theory

Phase diagrams for binary mixtures of 1,3-DAG do not exist in the literature; however, phase diagrams of binary TAG systems can provide some necessary background.

The main types of phase diagrams seen for TAG are depicted in Fig. 1 [1]. The formation of solid solutions (Fig. 1a) is the simplest case, where two crystal structures are so much alike that the crystal structure does not vary with changes in composition. Thus, neither component is subject to freezing point depression because neither component crystallizes as a pure compound (as stipulated by the Hildebrand equation) [20]. For TAG, solid solutions are formed when the two components have very similar melting points, molecular volumes and polymorphs. For example, binary mixtures 16:0–18:1c–18:0/18:0–18:1c–18:0 and 18:0–18:0–18:0/18:0–18:0–18:1t (where c and t indicate *cis* and *trans* bonds for oleic and elaidic acid) form solid solutions at all concentrations [1].

Eutectic systems (Fig. 1b) occur when the two components differ in molecular volume, shape or polymorph but still have similar melting points. Most binary mixtures of TAG display eutectic behavior [1]. The solid phase in these systems is considered to be a dispersion or mechanical mixture (a heterogeneous mixture which is, in principle, separable by mechanical means) of two solids: $S_A + S_B$ [7, 20]. For simplicity, this is often described as a suspension of pure A and pure B; however, in reality complete immiscibility does not occur and the solids are solid solutions rich in either component A (S_A) or component B (S_B) [7].

Another interesting feature of eutectic systems is the eutectic point (labeled in Fig. 1b). This point is the result of mutual freezing point depression between the two system components [20]. Regardless of the composition of the solid phase, the composition of the liquid first produced upon melting is defined by this point. For example, when melting is initiated (T slightly $> T_{eutectic}$) for binary mixtures with compositions either side of the eutectic, a solid (S_A or S_B) and a liquid phase of eutectic composition is the result. With further heating, the liquid phase becomes increasingly enriched in the main component of the solid solution. Complete melting yields a liquid phase with the composition of the binary mixture.

Monotectic systems (Fig. 1c) may be seen for binary mixtures of TAG with melting point differences as small as 20 °C (12:0–12:0–12:0/16:0–16:0–16:0); however, the difference in melting point is usually larger than this (e.g. >27 °C for 16:0-16:0-16:0/16:0-18:1-16:0) [1]. For a monotectic system, when a binary mixture in the liquid state is cooled, S_B crystallizes first, often far in advance of the lower-melting component. As this process continues, the concentration of the lower-melting component in the liquid phase increases, as it also must in the solid solution containing predominantly B (S_B). In binary mixtures of TAG the high-melting component usually dissolves 20 to 30% of the low-melting component [1].

Peritectic systems (Fig. 1d) are rare, occurring occasionally in mixed saturate/unsaturated TAG systems such as 16:0-18:1-16:0/16:0-18:1-18:1 [1].

Experimental Procedures

Materials and methods for the preparation of 1,3-DAG are the subject of a previous publication [21]. In short, diacid 1,3-DAG were prepared by reacting 1(3)-MAG with acid chlorides and triethylamine in the presence of 4-dimethylaminopyridine. Protected 1(3)-MAG precursors were synthesized by Dean-Stark condensation and free 1(3)-MAG was produced using an acidic cation exchange resin. The resulting MAG and DAG were purified by recrystallization or flash chromatography. The identity and purity of prepared compounds was determined by NMR and GC/FID, respectively [21]. All physical and chemical techniques used in this work, with one exception, have been described in a previous publication [22]. The preparation and determination of binary phase diagrams follows, since it has not been described previously. Phase diagram samples were prepared from 0.0833 M solutions of pure compounds dissolved in chloroform/ethyl acetate (1:1). Samples with proportions 1:9 (i.e. 100 + 900 μL), 2:8 (i.e. 200 + 800 μL), 3:7, 4:6 … 9:1 were prepared. Solvent was evaporated under a stream of nitrogen with mild heating

($\sim$40 °C) to compensate for enthalpy of vaporization. Once solvent had completely evaporated, 6–8 mg of each melted binary mixture was measured into an alodined aluminum DSC pans and sealed. Samples of pure 1,3-DAG were prepared and tested in the same manner to verify the method. Samples were stored at -30 °C for at least 16 h prior to analysis. DSC melting data was collected with a heating rate of 2 °C/min using a Q1000 DSC (TA Instruments, New Castle, DE) that was calibrated following the manufacturer's recommendations with a pure indium standard and a matched pair of sapphires. The sample cell was purged with dry nitrogen flowing at 25 mL/min. Heat flow was measured relative to an empty sealed DSC pan. Onset, peak and enthalpy of melting were determined using the Universal Analysis software package version 4.2E (TA instruments). For each binary mixture, the extrapolated onset of melting (T_e) for the lowest-melting peak and the peak maximum (T_p) for the highest-melting peak were plotted. The preferred measurement of melting temperature (T_m) is the extrapolated onset of melting temperature (T_e) because it has been shown to vary the least with heating rate. T_e is the temperature at which a tangent through the linear portion of the leading edge of the peak intersects with the baseline. In the event that T_e is not available, as is the case with multiple peaks and peaks that merge due to polymorphism, T_p is an acceptable approximation [23].

Results and Discussion

Six diacid 1,3-DAG were prepared using representative FA: hexanoic (6:0)—SCFA; lauric (12:0)—MCFA; palmitic (16:0)—LCFA; and oleic (18:1)—MUFA. For

Table 1 Melting data for diacid 1,3-diacylglycerols

1,3-DAG		T_e (°C)	T_p (°C)	ΔH_f (kJ/mol)
A 6:0-OH-12:0	β_1	22.42	25.89	52.49
	β_2	18.43	24.00	43.19
B 6:0-OH-16:0	β_1	33.36	35.67	
	β_2	12.95	26.61	
C 6:0-OH-18:1	β_1	-1.99	3.22	51.44
	β_2	-6.68	0.53	48.81
D 12:0-OH-16:0	β_1	58.84	60.96	108.08
	β_2	53.80	57.30	97.02
E 12:0-OH-18:1[a]	β_1	27.65	28.42	83.34
	β_2	22.90	27.40	83.12
F 16:0-OH-18:1	β_1	42.11	42.83	120.29
	β_2	36.51	40.64	112.21

[a] Data collected at 5 °C/min (others at 2 °C/min); literature value for T_m β_1 = 32 °C [24]

Fig. 2 DSC curves for a crystallization and d melting of 1,3-hexanoyl-lauroyl-*rac*-glycerol; b crystallization and e melting of 1,3-hexanoyl-oleoyl-*rac*-glycerol; and c crystallization and f melting of 1,3-lauroyl-oleoyl-*rac*-glycerol. Plots in each graph were measured at 10 °C/min (*top*), 5 °C/min (*middle*) and 2.5 °C/min (*bottom*). *Dashed line* (in Fig. 2f) indicates high-melting form melted at 5 °C/min
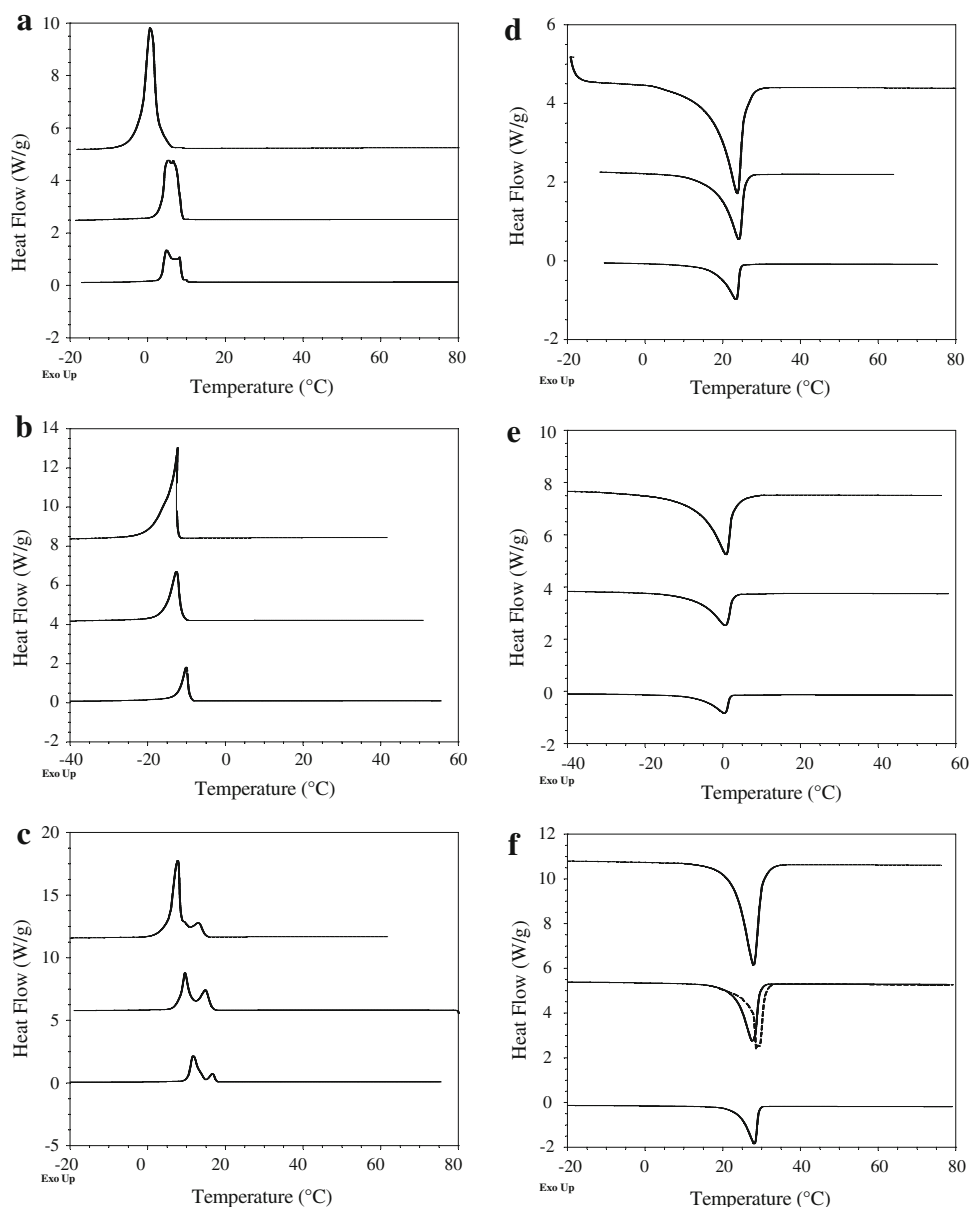
simplicity, a letter was assigned to each compound: (A) 1,3-hexanoyl-lauroyl-*rac*-glycerol (6:0-OH-12:0), (B) 1,3-hexanoyl-palmitoyl-*rac*-glycerol (6:0-OH-16:0), (C) 1,3-hexanoyl-oleoyl-*rac*-glycerol (6:0-OH-18:1), (D) 1,3-lauroyl-palmitoyl-*rac*-glycerol (12:0-OH-16:0), (E) 1,3-lauroyl-oleoyl-*rac*-glycerol (12:0-OH-18:1) and (F) 1,3-palmitoyl-oleoyl-*rac*-glycerol (16:0-OH-18:1). The preparation protocol (including TLC R_f and NMR data) for these compounds has been published [21] and the physical chemistry of three of these compounds (B, D and F) has been described [22]. The most-thermodynamically stable polymorph was obtained by storing each pure sample at −30 °C for at least 1 week, and was evaluated by DSC, XRD and FTIR. Samples were stored at −30 °C to minimize acyl migration [21]. The crystallization behavior of

the remaining three compounds (A, C and E), determined using published methodologies [22], is discussed briefly below.

Binary mixtures of the six compounds listed above were used to create phase diagrams, hereafter identified by the letter names of their two components, for example: AB (6:0-OH-12:0 and 6:0-OH-16:0); AC (6:0-OH-12:0 and 6:0-OH-18:1); AD (6:0-OH-12:0 and 12:0-OH-16:0)… EF (12:0-OH-18:1 and 16:0-OH-18:1).

Physical Chemistry of Diacid 1,3-DAG

1,3-Hexanoyl-lauroyl-*rac*-glycerol (A) (>99% by GC), 1,3-hexanoyl-oleoyl-*rac*-glycerol (C) (75.28% by GC) and 1,3-lauroyl-oleoyl-*rac*-glycerol (E) (94.25% by GC) were
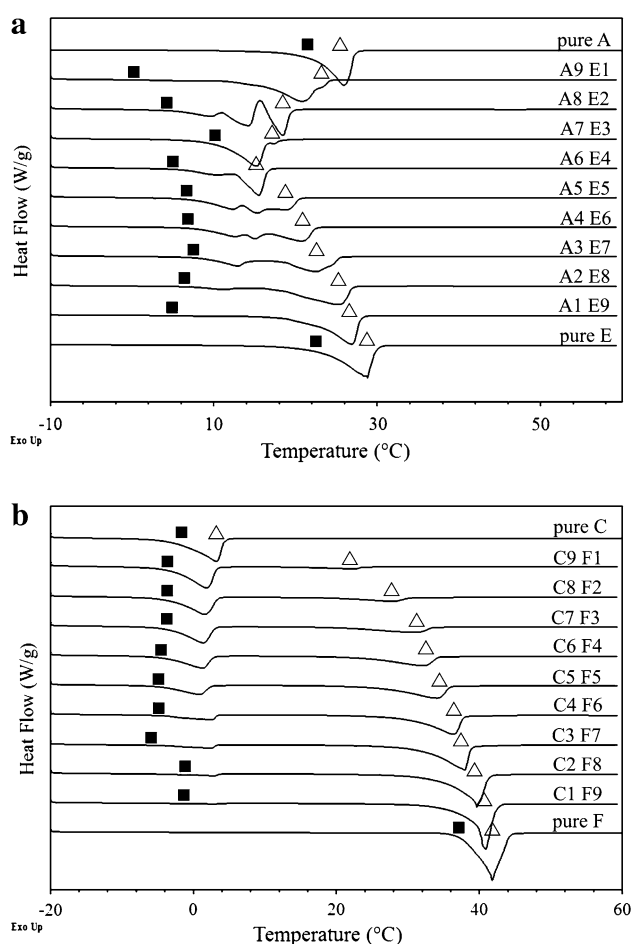
Fig. 3 DSC melting curves for binary blends of **a** A and E, and **b** C and F. Binary blends of compounds A 6:0-OH-12:0, C 6:0-OH-18:1, E 12:0-OH-18:1 and F 16:0-OH-18:1 are identified by their molar ratio (e.g. A9 E1 is 90% A and 10% E). Approximate location of T_e for first peak is marked with *filled squares* on the baseline. Approximate location of T_p for the final peak is marked with *open triangles* on the baseline

isolated by flash chromatography. Melting data for β_1 and β_2 forms of these compounds is listed in Table 1 and DSC curves are compiled in Fig. 2. Literature values are not available for 6:0-OH-12:0 or 6:0-OH-18:1 since they have not previously been reported in the literature (no CAS number). The melting point for 12:0-OH-18:1 ($T_e\ \beta_1 = 27.65\ °C$) is lower than the literature value (32 °C) reported for this compound [24]. Reasons for this, including differences in purity and methodology have been discussed in detail previously [22]. The occurrence of two peaks in DSC crystallization curves (at 5 and 2.5 °C/min for 6:0-OH-12:0 and at all cooling rates for 12:0-OH-18:1) is evidence of further polymorphism (beyond β_1 and β_2) (Fig. 2). This type of crystallization behavior is common for 1,3-DAG with moderate differences in acyl chain length [22]. Main peaks in XRD spectra for the high-melting forms of 6:0-OH-12:0 (4.63, 4.50, 3.83 and

3.78 Å) and 12:0-OH-18:1 (4.69, 4.58, 3.80 and 3.70 Å) are similar to those previously reported for the β_1 form of 12:0-OH-16:0 (4.63, 3.80 and 3.76 Å) [25] and for similar diacid 1,3-DAG [22]. The melting temperature of 6:0-OH-18:1 was too low to make XRD measurement feasible (aftermarket Peltier device limited to $\geq 5\ °C$).

Phase Diagrams

Samples were prepared and analyzed following the steps described above ("Experimental Procedures") and were held for a minimum of 16 h at −30 °C prior to analysis. This ensured that the most stable crystal forms had time to develop, and minimized acyl migration. A phase diagram is intended to depict the physical state of a blend of components at equilibrium. To approximate these conditions the slowest practical heating and cooling rates are used for data collection. For instance, in the current work a heating rate of 2 °C/min was used as recommended by Hohne, Hemminger and Flammersheim [23]. Crystallization requires undercooling to promote nucleation and, consequently, occurs at temperatures below the equilibrium melting point. For this reason, melting curves are preferred for the measurement of a sample's thermodynamic parameters [23]. Each melting curve was analyzed in the same manner described in "Experimental Procedures". Data (T_e, T_p and ΔH_f) was tabulated and the relevant points were plotted. The construction of phase diagrams is best illustrated by the following two examples (one eutectic, one monotectic).

Eutectic System

DSC melting curves for binary blends of A (6:0-OH-12:0) and E (12:0-OH-18:1) are compiled in Fig. 3 (Table 2). The relative concentration (molar) of each component in each sample is provided in the labels. For example, A4 E6 contains four parts component A (6:0-OH-12:0) and six parts component E (12:0-OH-18:1)—in other words, it is 0.6 mol fraction E. In Fig. 3, the approximate location of T_e of the first peak is marked by a filled square; the same symbol is used to mark the same point in Fig. 4d. Likewise, T_p of the final peak is marked by an open triangle; this symbol is also used to mark the same points in Fig. 4d. Interestingly, it is easy to recognize the eutectic system by simply including these points on a plot of compiled DSC curves (Fig. 3a).

In the melting curve for A8 E2 there are three endotherms (centered at 10, 14 and 18 °C) and one exotherm (centered at 16 °C) (Fig. 3a). These multiple peaks indicate the formation of meta-stable polymorphs (the exotherm was caused by the recrystallization of melted material into a more-thermodynamically stable polymorph). Whether this is due to the occurrence of two meta-stable polymorphs for the same solid solution of A and E, or the occurrence of

Fig. 4 Phase diagrams for binary mixtures **a** AB, **b** AC, **c** AD, **d** AE, **e** AF, **f** BC, **g** BD, **h** BE, **i** BF, **j** CD, **k** CE, **l** CF, **m** DE, **n** DF and **o** EF. *Capital letters* represent compounds as follows: *A* 1,3-hexanoyl-lauroyl-*rac*-glycerol (6:0-OH-12:0), *B* 1,3-hexanoyl-palmitoyl-*rac*-glycerol (6:0-OH-16:0), *C* 1,3-hexanoyl-oleoyl-*rac*-glycerol (6:0-OH-18:1), *D* 1,3-lauroyl-palmitoyl-*rac*-glycerol (12:0-OH-16:0), *E* 1,3-lauroyl-oleoyl-*rac*-glycerol (12:0-OH-18:1) and *F* 1,3-palmitoyl-oleoyl-*rac*-glycerol (16:0-OH-18:1). Symbols are: *Filled squares* T_e for the first peak; *open squares* T_p for a single peak and *open triangles* is T_p for the final peak
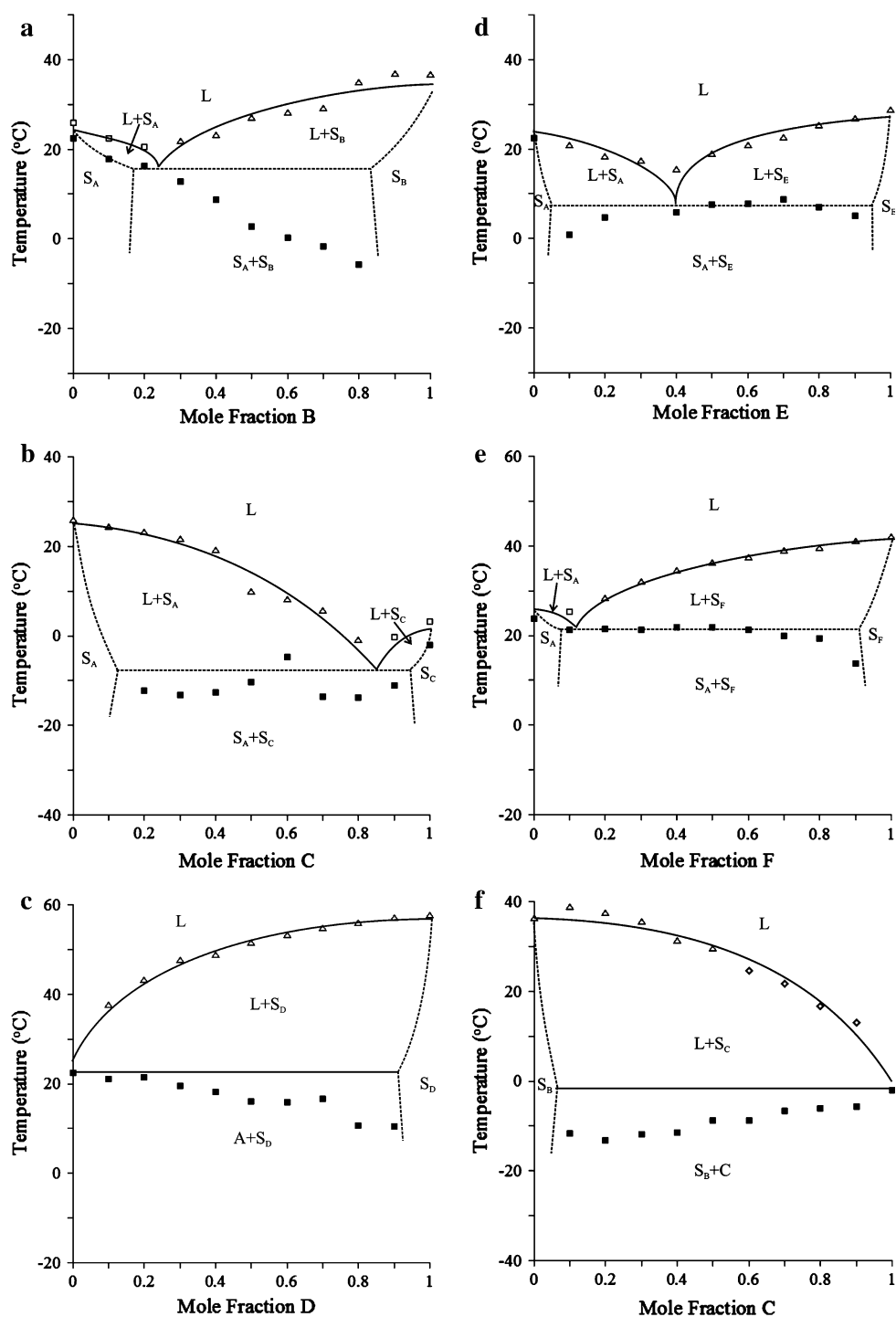

the same polymorphic form in two different solid solutions (e.g. solid solution *X* and solid solution *Y* with different melting points) is not known. To understand the source and mechanism for this occurrence would require further research and is beyond the scope of this study.

There is one major peak in the melting curves A7 E3 and A6 E4 (centered at ~15 °C) with a minor shoulder or side peak (Fig. 3a). This single major peak, along with the

persistence of this peak in other melting curves (i.e. A5 E5 and A4 E6) indicates eutectic formation. The melting of the eutectic gives rise to the middle peak in the DSC curves. Of course, this is obscured somewhat by peaks due to metastable polymorphs.

In these phase diagrams, the upper solid/liquid boundary (above which all material is liquid) is delineated by the liquidus line and the lower solid/liquid boundary (below

Fig. 4 continued
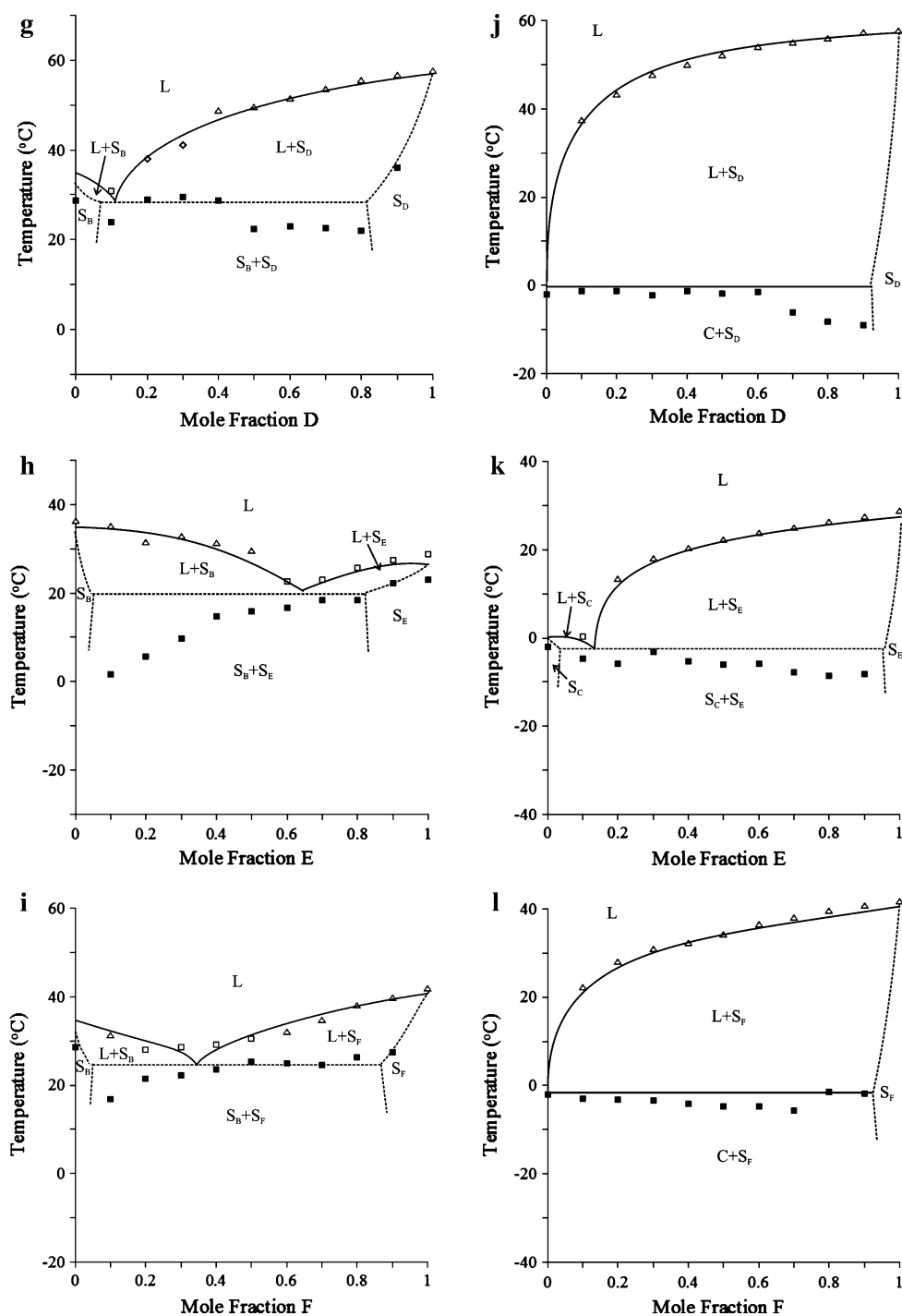
which all material is solid) is delineated by the solidus line [26, 27]. Under ideal conditions the solidus line should have a constant T_m with no melting occurring below this temperature. While the points obtained for binary phase diagram AE are typical, especially for the liquidus line, the solidus line deviates from ideal eutectic behavior (Fig. 4d). This is due to several contributing factors, one being the polymorphism discussed previously. In addition, as peaks become smaller, T_e changes due to the angle of the tangent

for the onset of melting which decreases the apparent melting point (Fig. 3a). This is a contributing factor to the lowering of T_e as measured in A9 E1, A8 E2, A2 E8 and A1 E9. Another factor is the presence of impurities; while A is >99% pure by GC, E had a purity of 94.25%. While this should have minimal impact on melting behavior for high concentrations of A, when A is present in low concentrations (i.e. 0.2 and 0.1 mol fraction), impurities in E will be present at relatively high concentrations (0.046 and

Fig. 4 continued
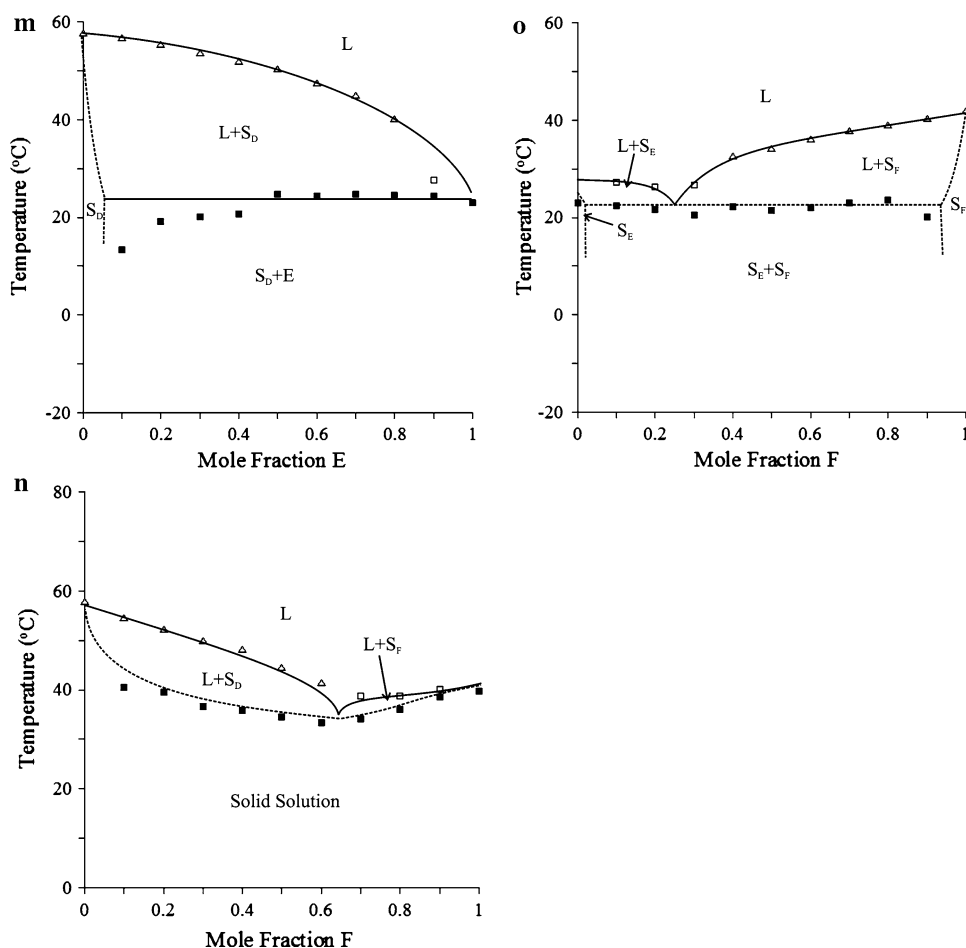
0.052 mol fraction, respectively) and, thus have a greater effect on melting point. This can be seen, to some degree, in all of the phase diagrams (Fig. 4), but, especially for (a) AB (x_B from 0.3 to 0.8), (h) BE (x_E from 0.1 to 0.7) and (m) DE (x_E from 0.1 to 0.4).

Monotectic System

DSC melting curves for binary blends of C (6:0-OH-18:1) and F (16:0-OH-18:1) are compiled in Fig. 3b. Points on the baseline for these curves have been marked in the same way as the previous example (filled squares for T_e of first peak; triangles for T_p of final peak). Similar to the eutectic system described above, the shape of the monotectic is visible in the placement of the labels for T_e and T_p (Fig. 3b). These labeled points were used to construct the phase diagram for CF binary blends (Fig. 4l). The melting point of the first peak remained fairly constant in this case; nevertheless, the measurement of T_e is affected by the decrease in size of the endotherm with decreasing x_C (C3 F7 to C1 F9; Figs. 3b and 4l) as discussed for AE.

Conclusions

Binary 1,3-DAG systems demonstrated either monotectic or eutectic behavior (Fig. 4). Consistent with TAG systems, the phase behavior of 1,3-DAG varied with the difference between the melting points of the two compounds in the binary mixture (ΔT_m) [1]. Thus, the monotectic systems ($\Delta T_m > 30$ °C) and the eutectic systems ($\Delta T_m <$ °C) were easy to distinguish. In addition, the position of the eutectic varied with ΔT_m, so that when $0 \leq \Delta T_m \leq 10$ °C the eutectic was between 0.40 and 0.25 (mole fraction of one component), when $10 \leq \Delta T_m \leq 20$ °C the eutectic was between 0.25 and 0.13, when $20 \leq \Delta T_m < 30$ °C the eutectic was between 0.14 and 0.10, and when $\Delta T_m > 30$ °C the systems were monotectic (Fig. 5). In the majority of the systems both components had one FA in common whereas for three of the binary mixtures (AF, BE and CD) the components had no common FA. Nevertheless, all diacid 1,3-DAG binary phase behavior could be categorized in this general way. In other words, complementarity of FA did not appear to play a role in phase behavior for the subject 1,3-DAG.

Table 2 Phase diagram summary

Figure	Components			ΔT_m	Behavior	Eutectic location	
	First		Second	(°C)		Exp.[c]	Calc.[c]
4a	AB	6:0-OH-12:0	6:0-OH-16:0	6.7	Eutectic	$x_B = 0.25$	0.3
4b	AC	6:0-OH-12:0	6:0-OH-18:1	24.41	Eutectic	$x_C = 0.85$	0.9
4c	AD	6:0-OH-12:0	12:0-OH-16:0	32.0	Monotectic	–	–
4d	AE	6:0-OH-12:0	12:0-OH-18:1	0.6	Eutectic	$x_E = 0.40$	0.3
4e	AF[a]	6:0-OH-12:0	16:0-OH-18:1	17.4	Eutectic	$x_F = 0.13$	0.1
4f	BC	6:0-OH-16:0	6:0-OH-18:1	31.1	Monotectic	–	–
4g	BD	6:00-OH-16:0	12:0-OH-16:0	25.3	Eutectic	$x_D = 0.10$	–
4h	BE[a]	6:0-OH-16:0	12:0-OH-18:1	6.1	Eutectic	$x_E = 0.65$	0.7
4i	BF	6:0-OH-16:0	16:0-OH-18:1	10.7	Eutectic	$x_F = 0.35$	0.15
4j	CD[a]	6:0-OH-18:1	12:0-OH-16:0	56.4	Monotectic	–	–
4k	CE	6:0-OH-18:1	12:0-OH-18:1	25.0	Eutectic	$x_E = 0.14$	–
4l	CF	6:0-OH-18:1	16:0-OH-18:1	41.8	Monotectic	–	–
4m	DE	12:0-OH-16:0	12:0-OH-18:1	31.4	Monotectic	–	–
4n	DF	12:0-OH-16:0	16:0-OH-18:1	14.6	Eutectic[b]	$x_F = 0.64$	0.9
4o	EF	12:0-OH-18:1	16:0-OH-18:1	16.8	Eutectic	$x_F = 0.25$	0.0

[a] Binary blends with no fatty acids in common

[b] Solids completely miscible

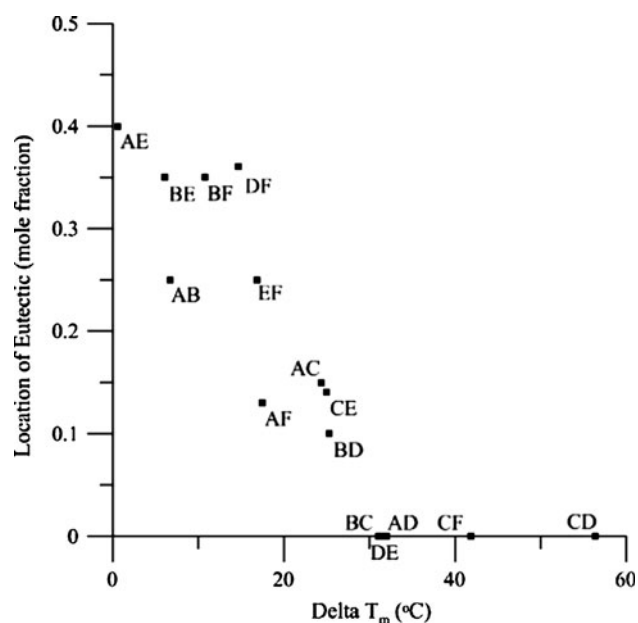[c] Experimental and calculated (Hildebrand equation) values

Fig. 5 Phase diagram summary—the location of the eutectic point in binary phase diagrams of 1,3-diacylglycerols is plotted versus the difference in melting temperature between the two components. Component definitions are provided in the description for Fig. 4. In this case, the eutectic point is the mole fraction of the nearest pure component in the phase diagram (i.e. mole fraction that is ≤ 0.5)

The development of these phase diagrams represents a preliminary step in understanding the phase behavior of 1,3-DAG. It has been possible to draw some general conclusions regarding the phase behavior of 1,3-DAG, such as the role of ΔT_m in determining phase behavior (eutectic or monotectic) on the basis of this study. However, further work will be required to better understand the phase behavior of 1,3-DAG in more complex systems.

References

1. Timms RE (1984) Phase behavior of fats and their mixtures. Prog Lipid Res 23:1–38
2. Barbano P, Sherbon JW (1978) Phase behavior of tristearin/trioctanoin mixtures. J Am Oil Chem Soc 55:478–481
3. Knoester M, De Bruijne P, Van Den Tempel M (1972) The solid–liquid equilibrium of binary mixtures of triglycerides with palmitic and stearic chains. Chem Phys Lipids 9:309–319
4. Gandolfo FG, Bot A, Floter E (2003) Phase diagram of mixtures of stearic acid and stearyl alcohol. Thermochim Acta 404:9–17
5. Inoue T, Hisatsugu Y, Yamamoto R, Suzuki M (2004) Solid–liquid phase behavior of binary fatty acid mixtures 1. Oleic acid/stearic acid and oleic acid/behenic acid mixtures. Chem Phys Lipids 127:143–152
6. Lambelet P, Raemy A (1983) Iso-solid diagrams of fat blends from thermal analysis data. J Am Oil Chem Soc 60:845–847
7. Lee AG (1977) Lipid phase transitions and phase diagrams II. Mixtures Involving Lipids. Biochim Biophys Acta 472:285–344
8. Abes M, Narine SS (2007) Crystallization and phase behavior of fatty acid esters of 1,3-propanediol I. Pure Systems. Chem Phys Lipids 149:14–27

9. Abes M, Bouzidi L, Narine SS (2007) Crystallization and phase behavior of 1,3-propanediol esters II. 1,3-Propanediol distearate/1,3-propanediol dipalmitate (SS/PP) and 1,3-propanediol distearate/1,3-propanediol dimyristate (SS/MM) binary systems. Chem Phys Lipids 150:89–108

10. Abes M, Bouzidi L, Narine SS (2008) Crystallization and phase behavior of fatty acid esters of 1,3-propanediol III. 1,3-propanediol dicaprylate/1,3-propanediol distearate (CC/SS) and 1,3-propanediol dicaprylate/1,3-propanediol dipalmitate (CC/PP) binary systems. Chem Phys Lipids 151:110–124

11. Flickinger BD, Matsuo N (2005) Diacylglycerols. In: Shahadi F (eds) Bailey's industrial oil and fat products. Wiley, Hoboken, pp 37–48

12. Inoue T, Hisatsugu Y, Ishikawa R, Suzuki M (2004) Solid–liquid phase behavior of binary fatty acid mixtures 2. Mixtures of oleic acid with lauric acid, myristic acid and palmitic acid. Chem Phys Lipids 127:161–173

13. Inoue T, Hisatsugu Y, Suzuki M, Wang ZN, Zheng LQ (2004) Solid–liquid phase behavior of binary fatty acid mixtures 3. Mixtures of oleic acid with capric acid (decanoic acid) and caprylic acid (octanoic acid). Chem Phys Lipids 132:225–234

14. Lerdkanchanaporn S, Dollimore D, Evans SJ (2001) Phase diagram for the mixtures of ibuprofen and stearic acid. Thermochim Acta 367–368:1–8

15. Biganska O, Navard P (2003) Phase diagram of a cellulose solvent: N-methylmorpholine-N-oxide-water mixtures. Polymer 44:1035–1039

16. Rai US, George S (1992) A physicochemical study on organic eutectics and addition compound; benzidine—pyrogallol system. Can J Chem 70:2869–2874

17. Rai US, Shekhar H (1994) Solidification behavior of binary organic eutectic alloys. Cryst Res Technol 29:533–542

18. Rai US, Rai RN (1998) Physical chemistry of organic eutectics. J Therm Anal 53:882–893

19. Ding MS, Xu K, Jow TR (2000) Phase diagram of EC-DMC binary system and enthalpic determination of its eutectic composition. J Therm Anal Calorim 62:177–186

20. White MA (1999) Properties of materials. Oxford University Press, New York

21. Craven RJ, Lencki RW (2010) Preparation of diacid 1,3-diacylglycerols. J Am Oil Chem Soc 87(11):1281–1291

22. Craven RJ, Lencki RW (2011) Crystallization and polymorphism of 1,3-acyl-palmitoyl-rac-glycerols. J Am Oil Chem Soc. doi:10.1007/s11746-01101769-0

23. Hohne GWH, Hemminger WF, Flammersheim HJ (2003) Differential scanning calorimetry. Springer, New York

24. Daubert BF, Longenecker HE (1944) Unsaturated synthetic glycerides. III. Unsaturated symmetrical mixed diglycerides. J Am Chem Soc 66:53–55

25. Sidhu SS, Daubert BF (1946) X-ray investigation of glycerides. V. Diffraction analyses of synthetic diacid diglycerides. J Am Chem Soc 68:2603–2605

26. Mullin JW (2001) Crystallization. Butterworth-Heinemann, Oxford

27. Atkins PW (1982) Physical chemistry. Oxford University Press, Oxford